ON DEVELOPMENT OF HIGH PERFORMANCE SAILS FOR AN OCEANGOING SAILING SHIP

Toshifumi Fujiwara (National Maritime Research Institute, JAPAN)
Koichi Hirata (National Maritime Research Institute, JAPAN)
Michio Ueno (National Maritime Research Institute, JAPAN)
Tadashi Nimura (National Maritime Research Institute, JAPAN)

Abstract: It is very important to reduce the ship's exhaust of carbon dioxide gas (CO_2) that is assumed to be one of causes of global warming on environmental problems all over the world. Sailing ships are able to decrease the ship's exhaust gas rather than conventional ships with a diesel engine. Then, we had the research to investigate efficiency of an oceangoing sailing ship. The research consists of the investigation of aerodynamic characteristics on hybrid-sails and performance of a hull form on the sailing ship, and assessment of the sailing performance of the ship. In this paper, the aerodynamic characteristics of the hybrid-sails consisted of a rigid wing sail, a slat and a soft sail are shown. The aerodynamic characteristics of them are very important for the ship because the sails on the deck have large effect on the sailing performance. The experiments on various kinds of the sails were carried out at the wind tunnel. As a result, the hybrid-sails presented in this paper are very useful compared with the previous sails equipped on the deck of ships actually. The performance of the aerodynamic characteristics is also confirmed by calculated results of CFD.

1. INTRODUCTION

The environmental destruction according to global warming in the entire earth is worried about because a large amount of use of the fossil fuel increases CO_2 in the atmosphere. In case of a ship, it will be effective to develop new technology on marine engines instead of the diesel engines in order to reduce exhaust gas. The thrust system using natural energy that might not make atmosphere dirty is also expected as the substitution of the diesel engines. It is examined to increase thrust by sails using the wind force in this paper.

The idea on use of the wind as the thrust of motor ships had been already presented when the fuel price of a ship soared about 20 years ago in oil crisis. Square rigid sails were installed in ships and the effectiveness of the equipped sails was confirmed in Japan. For example, the sailing ships built about 20 years ago are shown in Fig.1 [1] and Fig.2 [2]. The tanker in Fig.1, which is 66m in L_{PP}, has two square rigid sails that the total sail area is $200m^2$. The bulk carrier in Fig.2, which is 152m L_{PP}, also has two square rigid sails that the total sail area is $640m^2$. Those sails are a circular arc form.

Afterward, since the fuel price fell, the advantage of the equipped sails decreased in the higher cost of sail production, maintenance and operation. At present, the only one sail-equipped motor ship is plied in Japan except for small fishing vessels.

In this time, high performance of the aerodynamic characteristics on the sail is expected rather than that of those square rigid sails shown in Fig.1 and Fig.2 in smaller costs. In our research institute, various investigations of the aerodynamic characteristics on the sails were carried out in the wind tunnel [3]. The results of the hybrid-sails, which has the seriously effect on the sailing performance of the ship, are shown in this paper. The sail consists of the rigid wing sail, which plays a role of a mast, a slat and a soft sail as in Fig.3. The efficiency of this kind of the sails has already shown by Nojiri et al [4]. Finally it is confirmed that CFD is efficient measures to assess the performance of these kinds of sails.

A part of the results of the experiments in this paper has been used by Minami et al. [5] to assess the steady condition on sailing performance of an oceangoing sailing ship.

2. EXPERIMENTS

2.1 Experimental models

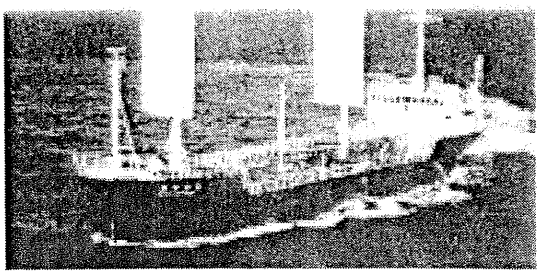

Fig.1 View of the sailing ship 'Shin Aitoku Maru'[1]

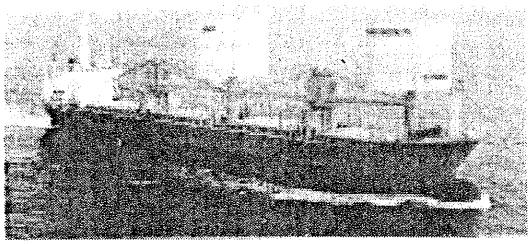

Fig.2 View of the sailing ship 'USUKI PIONEER' [2]

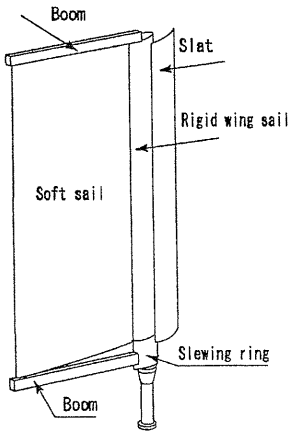

Fig.3 Basic concept of the high performance hybrid-sail

Fig.4 and Fig.5 show the size of the experimental models. In case of Fig.4, the model was named as the high mast sail. The rigid wing sail of NACA0030 type, which is 1.0m in height and 0.11m in width, was set up on the column mast that is 0.25m in height. The effect of the boundary layer on the floor can be ignored because of the sail's position. Two slats were made to investigate the effect of the size of them. The chord length and the circular arc radius of the slat are 0.1m, 0.1m named as the large slat and 0.05m, 0.1m named as the small slat respectively. The position of the slat is not translated, but the angle of that against

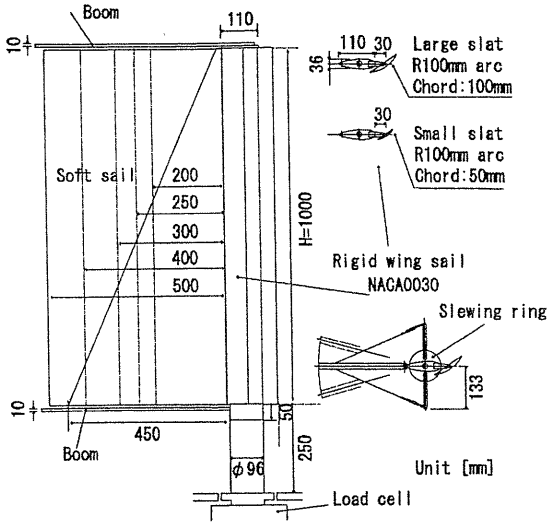

Fig.4 Experimental models on the high mast sail

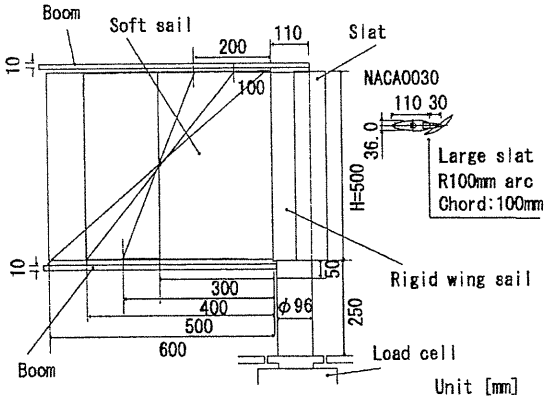

Fig.5 Experimental models on the low mast sail

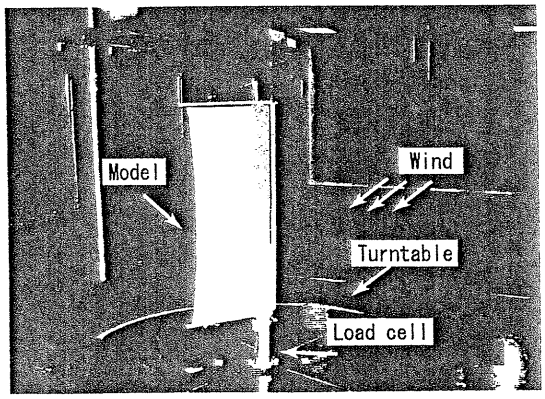

Fig.6 Experimental condition of the model

the sail can be changed. The square soft sails with a nylon, that are 1.0m in height and 0.2, 0.25, 0.3, 0.4, 0.5m in width and the triangular soft sail of 0.45m in base, were prepared for the experiments. This triangular hybrid-sail is shown in the reference paper [4].

In case of Fig.5, the model was named as the low mast sail. In the design stage of the sail, height of the sail that influences on the sail area is very important factor. According as the mast becomes tall, it is possible to have a large sail area, but there is restriction from the viewpoints of the stability and the manoeuvring in severe weather. Moreover, the port that can be used is limited in case of bulk carriers etc. because of the bridge near the port that the height is lower than that of the mast top of the sails. Therefore, the experiments using the low mast sail as in Fig.5 were carried out. Six soft sails were prepared to investigate the effect of the form and the width of the sails.

2.2 Experimental condition

The wind tunnel experiments were carried out in our research institute to investigate the aerodynamic characteristics of the sails. The experimental condition is shown in Fig.6. The load cell to measure forces and moment was set up to the center in the turntable and the sail model was jointed on the load cell. The wind velocity was uniform in the vertical direction, but the boundary layer about 0.1m existed on the floor in the tunnel.

2.3 Wind force and moment coefficients

Fig.7 shows the coordinate system of the model and definitions of forces and moment. The forces in the horizontal plane with respect to the wind is the drag force D, positive in the wind direction, and the cross force L, positive to the right when facing into the wind. The moment M for the vertical axis in the X-Y plane is the yawing moment. The α is the angle of the apparent wind based on the rigid wing sail. The β and the γ are the slat and the boom angle respectively.

The lift, drag forces and the moment coefficients are defined in non-dimensional forms as follows:

$$C_L = L/(1/2\rho_A U^2 S)$$
$$C_D = D/(1/2\rho_A U^2 S) \qquad (1)$$
$$C_M = M/(1/2\rho_A U^2 SC)$$

Here, ρ_A; density of air, U; velocity of wind, S; lateral projected area, C; chord length.

S is defined as the sum of the lateral projected area of the wing sail with the slat on the basis of X-axis at each setting and the area of the soft sail, that is, S slightly depends on the slat angle β. C is obtained from S/H, which H is height of the sail as in Fig.4 and Fig.5. The aspect ratio (AR) is defined as H^2/S.

The relationship between course direction of a ship and each wind force coefficient is shown in Fig.8. The thrust and side force coefficients C_X, C_Y, which have influence on the voyage of a ship, are defined as follows:

$$C_X = C_L \sin\theta - C_D \cos\theta$$
$$C_Y = C_L \cos\theta + C_D \sin\theta \qquad (2)$$

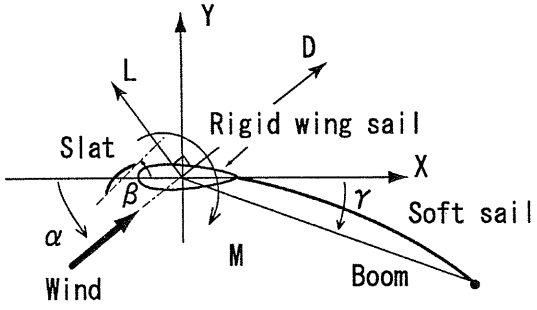

Fig.7 Coordinate system and definitions

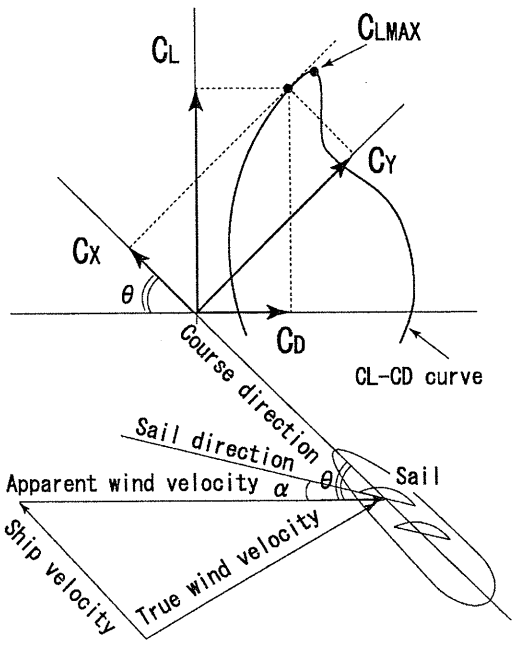

Fig.8 Relationship between course direction of a ship and thrust by the wind

2.4 Experimental results and discussions

All experiments were carried out in uniform steady flow. The wind velocity is 8m/s. In this case, the Reynolds number used the average chord of the model is about 2×10^5. It is confirmed that C_L and C_D are almost constant under the region of the Reynolds number. The list of the experiments is shown in Table 1. The results of each subject are shown in the figure from next sections.

Table 1 Experimental list

Subject	Case	Slat	RSH	SS	AR	Figure
Aspect ratio (High mast)	LH1	L	1000	Sq-200	2.63	Fig.9
	LH2			Sq-250	2.34	
	LH3			Sq-300	2.11	
	LH4			Sq-400	1.73	
	LH5			Sq-500	1.47	
	LH6			Tri-450	2.48	
Aspect ratio (Low mast)	LL1	L	500	Sq-300	1.06	Fig.10
	LL2			Sq-500	0.75	
	LL3			Sq-600	0.65	
Form of SS (Low mast)	LL1	L	500	Sq-300	1.06	Fig.11
	FLL1			Trape-400	1.06	
	FLL2			Trape-500	1.06	
	FLL3			Tri-600	1.06	
Parts	LH6	L	1000	Tri-450	2.48	Fig.13
	PH1	L	1000	non	-	
	PH2	non	1000	Tri-450	-	
	PH3	non	1000	non	-	
Slat	LH6	L	1000	Tri-450	2.48	Fig.14
	SH1	S	1000	Tri-450	2.64	

RSH; Height of Rigid Sail [mm], SS; Soft Sail, AR; Aspect Ratio, L; Large Slat, S; Small Slat, non; non-existance
[SS Column] Sq; Square Sail, Tri; Triangular Sail, Trape; Trapezium Sail, Number; Base length of the Soft Sail [mm]

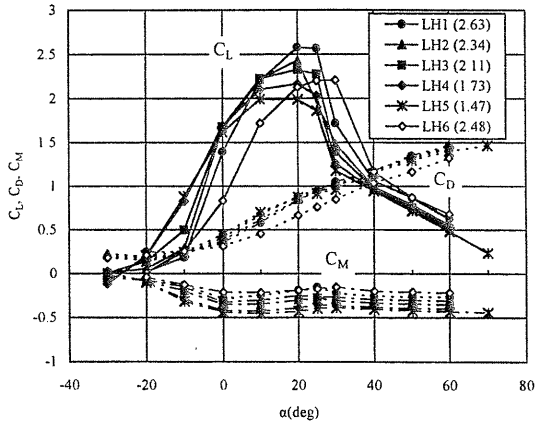

Fig.9 Aerodynamic characteristics of the high mast sail with different aspect ratios (AR=1.47~2.63, β=35deg, γ=30deg)

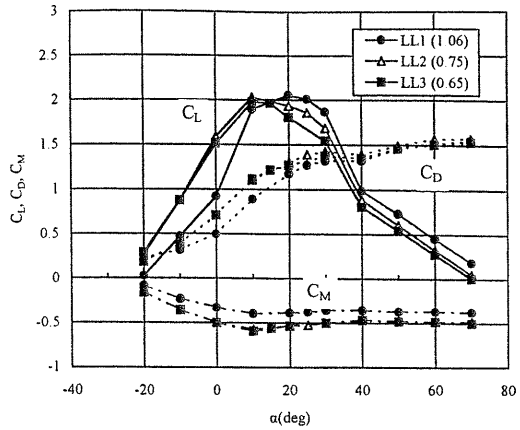

Fig.10 Aerodynamic characteristics of the low mast sail with different aspect ratios (AR=0.65~1.06, β=35deg, γ=30deg)

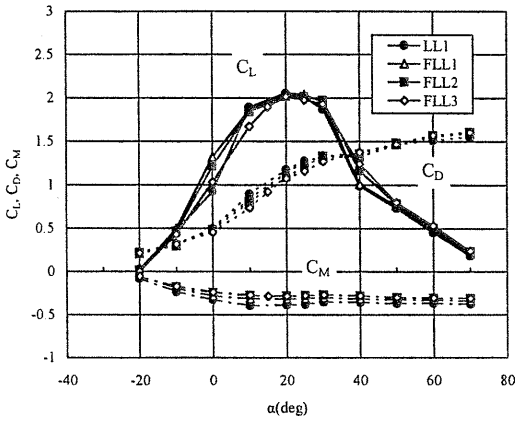

Fig.11 Aerodynamic characteristics of the low mast sail with different forms of the soft sail (AR=1.06, β=35deg, γ=30deg)

2.4.1 Aerodynamic characteristics with difference of aspect ratios

Aerodynamic characteristics of the high mast sail with difference of aspect ratios are shown in Fig.9 in case of the slat angle β=35deg, the boom angle γ=30deg. The setting on the slat and the boom bringing about higher lift was decided by previous experiments [3]. The results of the five kinds of the square soft sails and one triangular soft sail are shown in the figure. Number in the legend of the figure represents AR. It is understood that the lift force coefficients are greatly influenced by the aspect ratio though the drag coefficients are not greatly changed by them. The drag simply depends on the lateral area on the wing, that is, it is thought that the drag is dominated by the pressure drag at this Reynolds number. The maximum lift is recorded as 2.6 in case of LH1(AR=2.63). The lift of the square type sail is larger than that of the triangular one when those sails are same AR. From the viewpoints of the production, however, the triangular sail is superior to the square one.

Aerodynamic characteristics of the low mast sail with the difference of aspect ratios are shown in Fig.10 in case of the slat angle β=35deg, the boom angle γ=30deg as same as the previous figure. The results using three kinds of the square soft sails are shown in the figure. The maximum lifts are same level for the three models, but the values are smaller than those of the high mast sails i.e. the higher AR sails.

The effect of the soft sail forms is investigated as in Fig.11. The difference of C_L is observed in Fig.9 between the high mast sail of the square sail and the triangular sail that are same AR. In case of the low

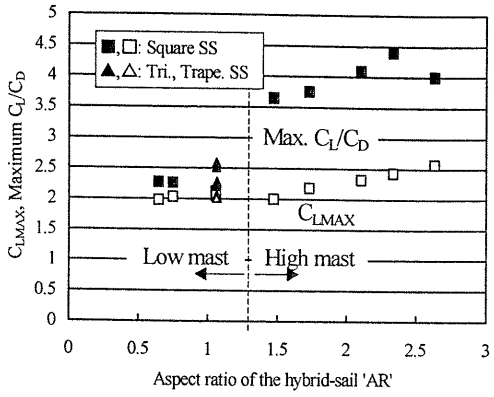

Fig.12 C_{LMAX} and maximum C_L/C_D (β=35deg, γ=30deg) [SS; Soft Sail]

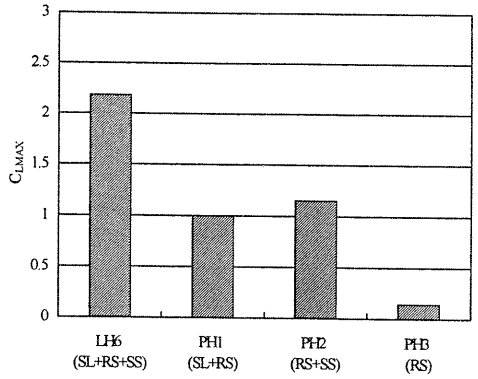

Fig.13 Effect of the parts on C_{LMAX} (β=35deg, γ=30deg) [SL; Slat, RS; Rigid Sail, SS; Soft Sail]

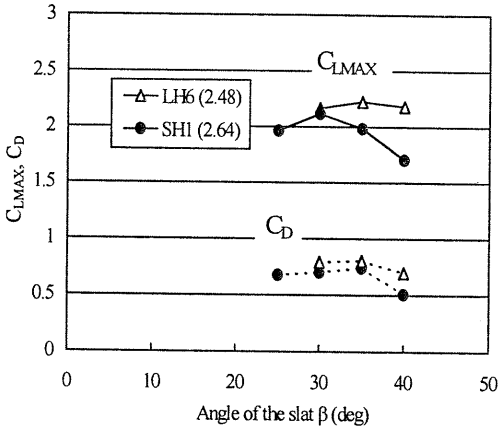

Fig.14 Effect of the slat angle on C_{LMAX} and C_D at C_{LMAX} (γ=30deg)

mast sails in Fig.11, the difference according to the soft sail form is very small compared with the case of the high ones. Bending of the soft sail is hardly given to the vertical direction for the low mast sail because the model size is relatively small. On the other hand, the tip line of the triangular soft sail of the high mast sail is observed to bend because of long sail length in vertical direction. This is thought as one of the reasons on C_L in between Fig.9 and Fig.11.

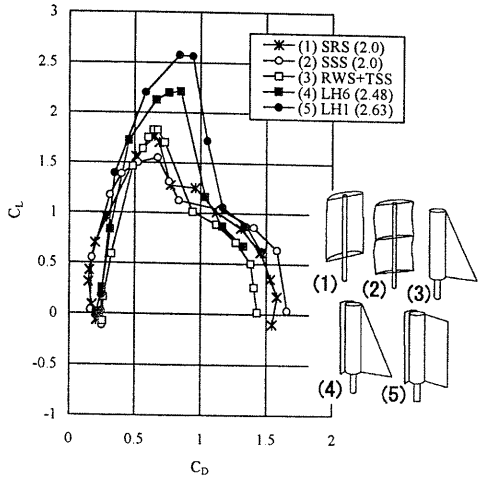

Fig.15 C_L-C_D curve on the various sails [SRS; Square Rigid Sail, SSS; Square Soft Sail, RWS; Rigid Wing Sail, TSS; Triangular Soft Sail]

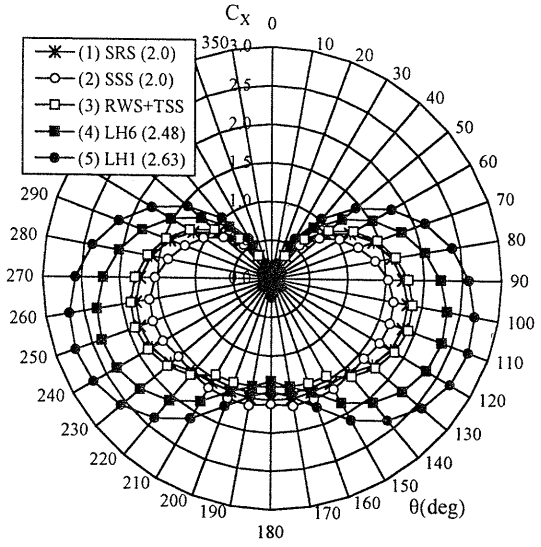

Fig.16 Polar curve of C_X on the various sails [SRS; Square Rigid Sail, SSS; Square Soft Sail, RWS; Rigid Wing Sail, TSS; Triangular Soft Sail]

Essentially, it is thought that the sail form influences on the induced drag broken out on the soft sail, but it is clarified that the influence of that is very small in the experiments.

2.4.2 C_{LMAX} and Maximum C_L/C_D

Fig.12 shows the maximum lift coefficients C_{LMAX} as open marks and the values of the maximum C_L/C_D as closed marks obtained from Fig.9~Fig.11. In case of an ordinary wing, the lift-curve slope and C_D/C_L^2 are usually used as the index of the performance of the wing. Here, the maximum C_L/C_D that influences on

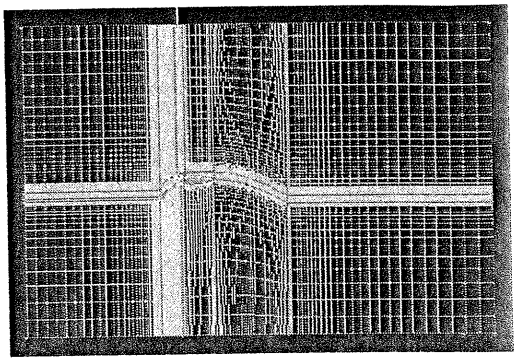

Fig.17 Grid example of the calculation on the hybrid-sail (LH2, β=35deg, γ=20deg)

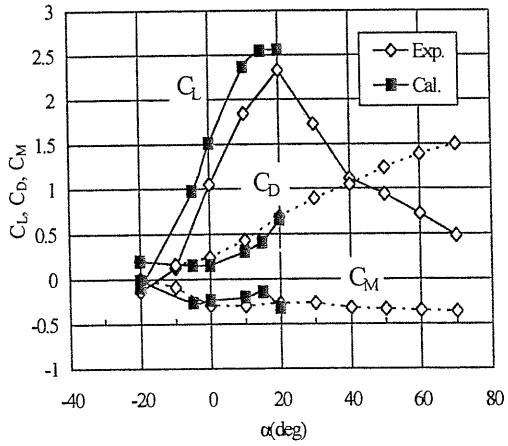

Fig.18 Aerodynamic characteristics of the hybrid-sails comparing the calculation results with the experimental ones (LH2, β=35deg, γ=20deg)

the performance of sailing on the wind is shown in the figure. The horizontal axis of the figure shows the aspect ratio AR.

Practically C_{LMAX} and the maximum C_L/C_D increase as the AR increases. This is the same tendency that the conventional wings of higher aspect ratio are observed to have higher lift-curve slope [6].

2.4.3 Effect of the slat, the rigid wing sail and the soft sail

The effect of the each element on C_{LMAX} is investigated using the LH6 model. The C_{LMAX} of PH1 and PH2 are same level. That of PH3 is very small compared with the others. This figure shows the lift of the hybrid-sail is mainly caused by the slat and the soft sail, and the influence of the slat is very large though the lateral project area of the slat is about half of that of the soft sail.

2.4.4 Size effect of the slat

It was clarified that the influence of the slat is very large from Fig.13. It is preferable, however, that the slat size is as small as possible when the sail is equipped with the slat actually from the structural viewpoint. Hence, the influence of the slat size was investigated. Fig.14 shows the result of C_{LMAX} and C_D at C_{LMAX} in case of the sails with the large slat and the small one. As shown in Table 1, LH1 equips with the large slat that has 0.1m chord and 0.1m circular arc. SH1 equips with the small slat that has 0.05m chord and 0.1m circular arc. Each different lateral projected area S is used in Eq.1. As a result, there is no large difference on C_{LMAX} between LH6 and SH1. Although C_{LMAX} of SH1 may decrease and the difference may become large in case of the same AR as shown in Fig.12, it is clear that even the small slat is efficient.

2.4.5 Comparison of the experimental results on the various sails

Fig.15 shows the comparison between the results of the present experiments and those of the previous sails already presented [7]. No.1 in the figure is the square rigid sail. No.2 is the square soft sail and No.3 is the rigid wing sail with a triangular soft sail. The AR of three kinds of the sails is about 2. The lift coefficient of No.5(LH1) presented in this paper is much larger than that of No.1~4.

Fig.16 shows C_X value at the polar graph on the sails shown in Fig.15. Maximum thrust coefficient of No.5(LH1) is about 2.7 in 110deg wind direction. The important point to gain the large thrust when $90deg<\theta<180deg$ is that the lift is not only large, but the drag is also large as in the equation (2). However, even if the aspect ratio was changed in this experiment results, a big difference was not seen in the drag coefficient either in Fig.9. Therefore, it is necessary to increase the lift coefficient by enlarging the aspect ratio as much as possible to gain the much thrust. The hybrid-sail presented in this paper is shown to have high performance on the thrust, but the mechanism of the sail is a little complex compared with the previous square sails.

3. CFD CALCULATIONS

When a new type sail is examined like this time, there are many combinations of parts and positions in order to seek the best performance of the sail, and it is difficult to cover all characteristics of them by the model experiments. It is in the current state that examinations of the aerodynamic characteristics can be carried out comparatively easily by CFD calculation. Therefore, the lift and the drag of the square hybrid-sail used in the experiments were calculated to confirm efficiency of CFD in deciding

the specification of the sail, and the results were compared with those of the experiments.

3.1 Numerical method

The calculations were carried out using packaged software 'Storm/CFD2000' supplied by Adaptive Research[8]. 'Storm' is a general-purpose computer program designed to numerically solve the Navier-Stokes equations, which consist of conservation equations for mass, momentum and energy.

3.2 Governing equations

The conservation of mass and Newton's second law applied to the fluid passing through a small fixed fluid volume are expressed as follows:

$$\frac{\partial \rho}{\partial t}+\frac{\partial(\rho u_i)}{\partial x_i}=0 \qquad (3)$$
$$\frac{\partial(\rho u_i)}{\partial t}+\frac{\partial(\rho u_i u_j)}{\partial x_j}=\frac{\partial \tau_{ij}}{\partial x_j}-\frac{\partial p}{\partial x_i}+\rho B_i$$

where ρ; fluid density, t; time, x_i; position vector in the ith coordinate direction, u_i; ith-fluid velocity component, B_i; component of the total body force per unit volume, p; local pressure, and τ_{ij} is the viscous stress tensor given by

$$\tau_{ij}=\mu\left[\left(\frac{\partial u_i}{\partial x_j}+\frac{\partial u_j}{\partial x_i}\right)-\frac{2}{3}\delta_{ij}\frac{\partial u_k}{\partial x_k}\right] \qquad (4)$$

Here, μ; dynamic viscosity of the fluid due to laminar diffusion, δ_{ij}; the Kronecker delta function.

3.3 Algorithm

The code uses a finite-volume representation of the governing equations. 'Storm' uses the PISO (Pressure Implicit with Splitting of Operators) algorithm developed by Issa [9] and Issa et al. [10] to solve the coupled system of governing equations. The solution algorithms chosen for the flow solver were incomplete LU decomposition for pressure and the Alternating Direction Implicit (ADI) method for all flow velocities. The convective terms in the governing equations were modeled using a second-order up-wind scheme which discrete using central differencing. The diffusive terms were modeled using an arithmetic mean interpolation scheme for evaluation of the transport coefficients between cell faces.

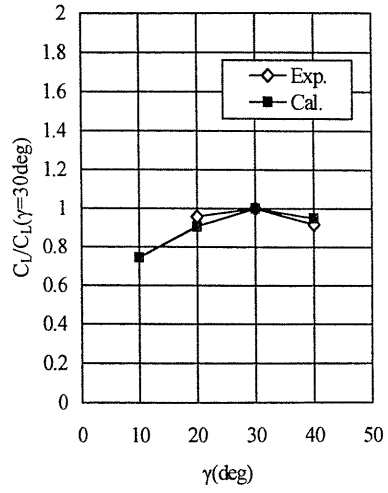

Fig.19 Comparison between the calculation results and the experimental ones on relative C_L in case of the different boom angle (LH2, α=20deg, γ=30deg)

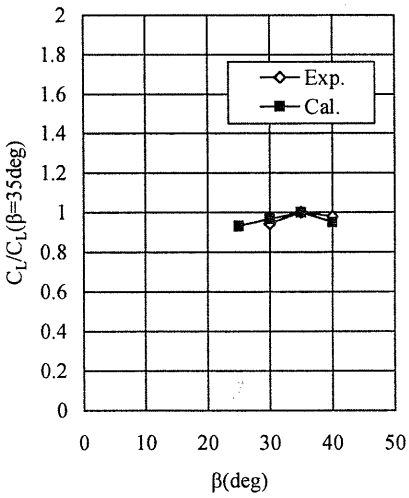

Fig.20 Comparison between the calculation results and the experimental ones on relative C_L in case of the different slat angle (LH2, α=20deg, γ=30deg)

3.4 Model description

The LH2 sail was used in the calculation. As for example, the model geometry and the mesh are shown in Fig.17. From the specification of the target hybrid-sail, 2-D calculation was done using BFC grid in this paper. The coordinate and the definitions are defined as same as the previous section. The soft sail has average curvature in the vertical obtained from the three-dimensional measurement using stereovision. The flow domain of the model is 3.5C long in the X-direction, 2.3C long in the Y-direction

as the representative length C that is the total sail chord. The flow domain was divided into six sections in the X-direction and five sections in the Y-direction. The mesh was stretched towards the sail to increase cell density near the sail and it contains 170 cells in the X-direction, 120 cells in the Y-direction for a total of 20400 cells.

3.5 Boundary and calculation conditions

The flow was computed by the laminar solution. No slip condition is given on the sail surface. The density was based on the ideal gas. The Reynolds number is 2.2×10^5 in the 8.0 m/s wind velocity as same as the experimental condition. The constant for 1.0×10^{-4} seconds at time interval was used and the duration time is 1.5~2 seconds in the calculation when the steady solution has been obtained.

3.6 Calculated results

The calculated results were compared with the experimental ones as shown in Fig.18. The open diamonds stand for the experimental and the closed squares for calculated results in the figure. The calculated results are in the overestimation because of not including the 3-dimensional effect of the sail, but the tendency between experimental results and calculated ones agrees with each other.

The influence of the boom angle and the slat angle was investigated in the calculations. We have already gotten the results that the influence of the bend of the sail is very small. Hence, in these cases, the calculations were done by the condition that the sail is flat. The results were compared with the experimental ones in Fig.19 and Fig.20 by a relative evaluation. The maximum values are obtained at γ=30deg in Fig.19 and at β=35deg in Fig.20. As a result, CFD is very useful to investigate the performance of these kinds of sails because the experimental results and calculated results have same tendency on the maximum lift coefficient.

4. CONCLUSIONS

As the reference of the future work to build the oceangoing sailing ship, the aerodynamic characteristics of the hybrid-sails were investigated experimentally and computationally. The results may be summarized as follows:

(1) The effectiveness of the present hybrid-sails consisting of the rigid wing sail, which plays the role of a mast, the slat and the square soft sail was confirmed by comparing with the previous sails.

(2) The lift coefficient almost increases as the aspect ratio increases in the experiments. On the other hand, the drag coefficient does not change largely in that case.

(3) The influence of the slat and the soft sail on aerodynamic characteristics was investigated in the experiments. It was understood that the influence of the slat on the lift is very large.

(4) The maximum lift coefficient was obtained as 2.6 and the maximum thrust coefficient as 2.7 by the optimum setting of the hybrid-sail.

(5) It was shown that CFD is very useful to investigate the performance of the hybrid-sail by relative evaluation even if the sail has complex shape like this time.

ACKNOWLEDGEMENTS

The authors are greatly indebted to Dr. Kunihiro Hoshino in our research institute for measuring the sail surface curvature in the wind by the three-dimensional measurement using stereovision.

REFERENCES

[1] Matsumoto N., Inoue M. and Sudo M. "Operating Performance of a Sail Equipped Tanker in Wave and Wind", Second International Conference of Stability of Ships and Ocean Vehicles (STAB), pp451-464, 1982

[2] Usuki Iron Works Ltd "International Voyage Sail-equipped Bulk Carrier 'USUKI PIONEER' ", Funenokagaku, Vol.38, pp36-43, 1985 (in Japanese)

[3] Fujiwara T., Hirata K., Ueno M. and Nimura T. "On Aerodynamic Characteristics of a Hybrid-Sail with Square Soft Sail", The Proceedings of the Thirteenth International Offshore and Polar Engineering Conference (ISOPE2003), Hawaii, USA, 2003

[4] Nojiri T., Sano K., Yagi H., Inoue H. "Hybrid Sail developed to show Max. Lift coefficient of 2.42 for Large Vessels -Reduction of Fuel Consumption and CO_2 Gas Emissions Expected-", MITSUI ZOSEN TECHNICAL REVIEW, No.178, pp.132-138, 2003

[5] Minami Y., Nimura T., Fujiwara T. and Ueno M. "Investigation into Underwater Fin Arrangement Effect on Steady Sailing Characteristics of a Sail Assisted Ship", The Proceedings of the Thirteenth International Offshore and Polar Engineering Conference(ISOPE2003) , Hawaii, USA, 2003

[6] Abbott I.H. and Doenhoff A.E.V. "Theory of Wing Sections", Dover Publications Inc., 1959

[7] Ishihara M., Watababe T. et al "Prospect of Sail-Equipped Motor ship as Assessed from Experimental Ship 'Daioh' ", Shipboard Energy Conservation Symposium, The Society of Naval Architects and Marine Engineers, pp181-198, 1980

[8] Adaptive Research, http:// www.adaptive-research.com or Fluid Technology Co. Ltd. in Japan, http://www.fluid.co.jp., 1997
[9] Issa R.I. "Solution of the Implicitly Discretized Fluid Flow Equations by Operator-Splitting", Journal of Computational Physics, Vol.62, pp40-65, 1985
[10] Issa R.I., Ahmadi-Befrui B., Beshay K.R. and Gosman A.D. "Solution of the Implicitly Discretized Reaching Flow Equations by Operator-Splitting", Journal of Computational Physics, Vol.93, pp388-410, 1991.

AUTHOR'S BIOGRAPHY

Toshifumi Fujiwara is the Chief Researcher, Manoeuvring and Control Group, Department of Maritime Safety, National Maritime Research Institute (NMRI), Japan.
1994: Researcher, Planning Department, Ship Research Institute (SRI), Ministry of Transport, Japan
1995: Researcher, Ship Dynamics Division, SRI
1998: Chief, Safety Standards Division, Maritime Technology and Safety Bureau, Ministry of Transport, Japan
2000: Researcher, Ship Dynamics Division, SRI
2002: the present post